

Cross Polarized 2×2 UWB-MIMO Antenna System for 5G Wireless Applications

Haitham Alsaif^{1,*}, Muhammad Usman¹, Muhammad T. Chughtai¹, and Jamal Nasir²

Abstract—A novel cross polarized compact antenna system is proposed for Ultra Wide Band communications. It also covers the sub-6 GHz band for initial 5G launch. The overall antenna system is a distinctive combination of Multiple Input Multiple Output (MIMO) antenna system covering radio frequency (RF) band starting from 2 GHz to 12 GHz. This MIMO system consists of two F-shaped monopoles with slotted fractured ground planes. The two antennas are fabricated back to back with 90 degree difference. The overall volume of the MIMO antenna system is 14 mm × 14 mm × 0.25 mm. Due to its very compact design, it is suitable for mobile phones and other hand-held devices. The peak measured gain has been achieved as 4.8 dB, and the measured far field patterns are nearly isotropic. Envelope Correlation Coefficient (ECC) and Gain Diversity are presented for the proposed MIMO antenna system.

1. INTRODUCTION

In recent years, an exponential increase in data rate is required by new generation of smart phones and a range of other hand-held wireless devices, which has given rise to new challenges for communication system industry. Long term evolution (LTE) in 4G commercial services is at the brink of meeting these new high data rate requirements. Currently, in order to overcome this problem the industry is launching a sub-6 GHz, 5th Generation (5G) mobile devices, whereas it is planned to use existing LTE network, and later on it will shift to millimeter band (28 GHz to 85 GHz) by 2020 [1–4].

By aiming this new challenge of increasing data rate, a novel 2×2 UWB-MIMO antennas system for mobile devices is presented in this article. It has been designed, fabricated and tested to evaluate and conform its performance. The designed antennas system covers the radio frequency band from 2 GHz to 12 GHz, which meets IEEE 802.11 a/b/g/n/ac standards including sub-6 GHz 5G bands. Furthermore, this compact UWB-MIMO antenna system satisfies the operating regulations of Federal Communication Commission (FCC) for UWB communication systems [5, 6]. This designed antenna system, due to its very compact design, stands out as an ideal candidate for the use in UWB, Wi-Fi and sub-6 GHz, i.e., 5G mobile devices.

At present, MIMO antenna systems are vastly used in wireless devices to increase data rate [7, 8]. Recently, the UWB and MIMO technologies are integrated together in wireless devices to increase the channel capacity in multipath propagation environment [9–12]. Among many challenges, a big challenge has been faced while designing the MIMO systems is its large volume which helps in reducing the coupling between antennas. Reduction in inductive coupling of antennas can be achieved by enlarging the distance between antenna elements hence resulting in increased volume of antenna system [13]. An alternative way to achieve reduced values of coupling between antenna elements is to incorporate cross

Received 11 October 2018, Accepted 21 November 2018, Scheduled 7 December 2018

* Corresponding author: Haitham Alsaif (h.alsaf@uoh.edu.sa).

¹ Electrical Engineering Department, College of Engineering, University of Hail, Saudi Arabia. ² Department of Electrical Engineering, COMSATS Institute of Information Technology, Abbottabad, KPK, Pakistan.

polarized antenna geometries [14, 15]. Polarization diversity results in complex antenna designs leading to compact antenna volumes [16–21].

This paper presents the use of polarization diversity technique to achieve compact design of the antenna system. The design consists of two ‘F’ shaped antennas using slotted fractured ground planes. The two antenna systems are fabricated in a back to back configuration but having cross polarized symmetry.

2. ANTENNA DESIGN METHODOLOGY AND PARAMETRIC STUDY

This section presents antenna design methodology which is followed by a parametric study.

2.1. Antenna Configurations

Geometrical arrangement of the antenna under consideration and design parameters for dual-port UWB MIMO are shown in Figure 1. It comprises two printed monopoles on the opposite sides of a low cost FR4 substrate having relative permittivity (ϵ_r) value of 4.6, and loss tangent ($\tan \delta$) value of 0.0025. The slotted ground planes were imprinted on opposite sides of the same substrate. The overall achieved measured dimensions of the proposed UWB MIMO antenna were only $14 \times 14 \text{ mm}^2$. The dimensions of radiator elements and ground planes are detailed in Table 1.

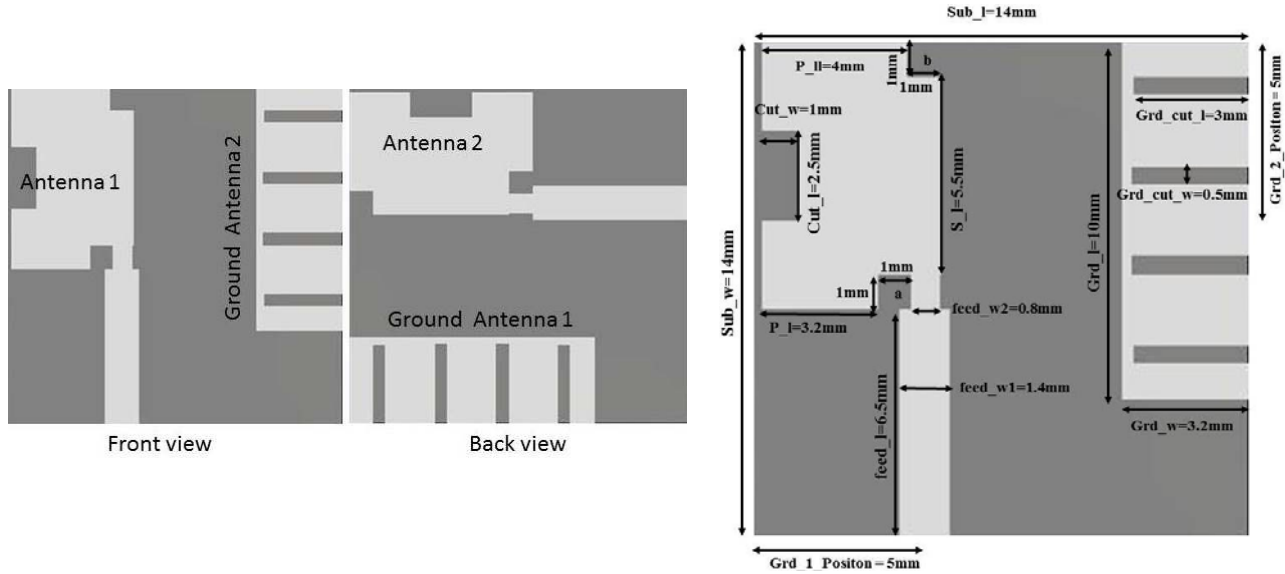


Figure 1. Geometry of the proposed MIMO antenna.

Table 1. Parameters of designed UWB MIMO antenna as shown in Figure 1.

Parameter	<i>a</i>	<i>b</i>	<i>Sub_l</i>	<i>Sub_w</i>	<i>feed_l</i>	<i>feed_w1</i>	<i>feed_w2</i>	<i>P_l</i>	<i>S_l</i>
value (mm)	1×1	1×1	14	14	6.5	1.4	0.8	3.2	5.5
Parameter	<i>Cut_l</i>	<i>Cut_w</i>	<i>P_ll</i>	<i>P_ll</i>	<i>Grd_l</i>	<i>Grd_cut_w</i>	<i>Grd_cut_l</i>	<i>Grd_w</i>	
value (mm)	2.5	1	3.2	4	10	0.5	3	3.2	

Generally in the case of a UWB antenna, obtaining a compact size and cutoff frequency in lower region, i.e., 3.1 GHz, is basic requirement. In order to fulfill these requirements, an appropriate radiating structure becomes a necessity. In this work, a monopole structure has been selected to develop a reduced UWB MIMO system. In the case of monopole, the resonance frequency in lower region can easily be

obtained by using the following equation [22]:

$$f_r = \frac{14.4}{l_1 + l_2 + g + \frac{A_1}{2\pi\sqrt{\varepsilon_r + 1}} + \frac{A_2}{2\pi\sqrt{\varepsilon_r + 1}}} \quad (1)$$

In Equation (1), l_1 and l_2 denote ground plane ($\text{Grd_}l = 10 \text{ mm}$) and radiator patch length ($\text{Sub_}w = 14 \text{ mm}$), respectively; A_1 is the ground plane area; and A_2 is the radiation patch area, while g (thickness of substrate 0.25 mm) is the gap between radiation patch and ground plane.

The radiating patches of the proposed UWB MIMO antenna system are designed in an F-shape having central rectangle of length 7 mm and width 5 mm. The two radiators were etched on the opposite sides of substrate. The radiators are fed with step-shaped microstrip having feedline size of $\text{feed_}l \times \text{feed_}w_1$. A step $\text{feed_}w_2$ (0.8 mm \times 1 mm) has been created in the feed line to improve impedance matching. Modified ground planes ($\text{Grd_}l \times \text{Grd_}w$) were also etched on the opposite sides of antenna substrate. In order to improve the matching and increase the operating bandwidth of the proposed antenna small notches of size $\text{Grd_cut_}w \times \text{Grd_cut_}l$ are etched on both the ground planes. As the two radiators are on the opposite sides of antenna substrate and have separate ground planes, mutual coupling is quite low within the whole band of operation.

The presented antenna design results from evolution of different geometries as shown in Figure 2. In Figure 2, Antenna i shows a step feed line which feeds a rectangular radiating element on one side of antenna substrate while the modified plane of ground as shown in Figure 4 (Ground iii) has been etched on the other side of the substrate. It can be observed from Figure 4 that with this type of configuration, the required UWB bandwidth could not be achieved. Therefore, the radiator was modified by decreasing its size as depicted in Figure 2 (Antenna ii). Due to reduction in size, the matching has been improved in the lower UWB range, but the matching at the upper frequency range of UWB is still poor. In order to improve the matching in the upper UWB range, a small notch is introduced on the right middle part of of Antenna ii configuration in Figure 2 and is shown in Figure 2 as Antenna iii. A parametric study has also been done on the length of this notch ($\text{Cut_}l$) which showed nonsignificant effect on S_{11} as can be witnessed from Figure 3. Based on these results, Antenna iii is chosen as the required radiator in the case of the proposed UWB MIMO antenna.

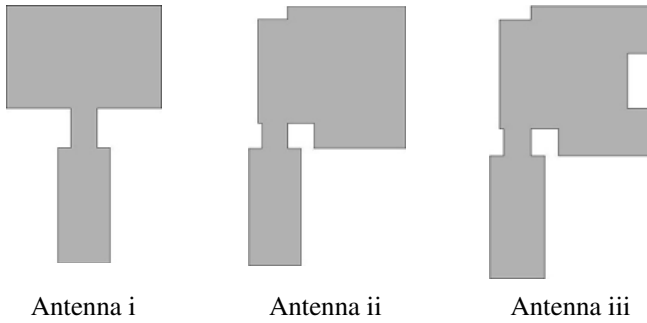


Figure 2. Different radiator shapes from which the proposed antenna was evolved.

2.2. Effect of Ground Plane on Antenna Performance

The ground plane plays a significant role in terms of impedance matching for the proposed design of UWB MIMO antenna. Figure 4 shows step by step evolution of ground plane for the proposed antenna. In scheme for ground as mentioned in Figure 4, Ground i represents a complete ground plane having a length equal to the length of the substrate, i.e., 14 mm, whereas in Figure 4 Ground ii shows a reduction in length ($\text{Grd_}l$) from 14 mm to 10 mm. Also in Figure 4, Ground iii, small notches ($\text{Grd_cut_}l \times \text{Grd_cut_}w$) have been introduced to achieve improved coupling and better response in UWB range. Figure 5 presents S_{11} for different ground configurations. By observing Figure 5, it is evident that for Ground i the bandwidth is very narrow, and the matching above 4 GHz is very poor. A resonance can be seen at 3 GHz. To help improve the bandwidth, the length ($\text{Grd_}l$) of the ground plane is reduced

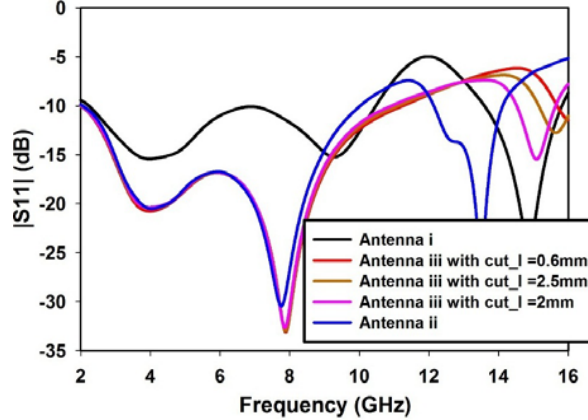


Figure 3. S_{11} (Simulated) for different radiators configuration.

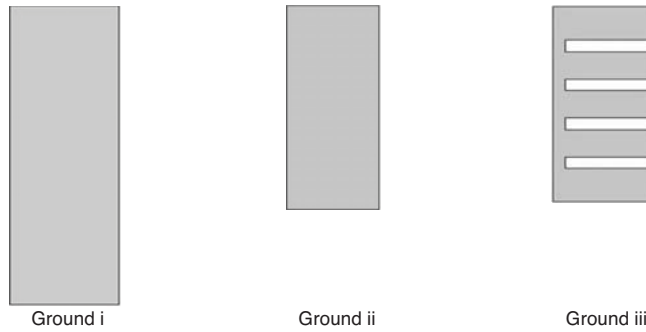


Figure 4. Different Radiator Shapes from which the proposed antenna is evolved.

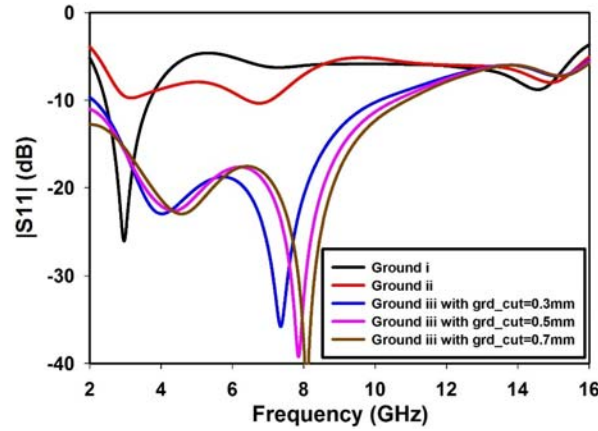


Figure 5. S_{11} (Simulated) for different radiators configuration.

to 10 mm (Ground ii). This resulted in an additional resonance at around 7 GHz in addition to the resonance at 3 GHz (Figure 5). However, the matching was still recognized poor within the whole band. To improve matching, rectangular notches of size Grd_cut_l \times Grd_cut_w were created in the ground plane (Ground iii). This resulted in an improved matching throughout the band of interest as shown in Figure 5. Also, notch width (Grd_cut_w) was forced to undergo the parametric study. Increase in the notch width resulted in an increase in bandwidth of the proposed antenna, as can be seen in Figure 5. Figure 5 only shows the S_{11} because the two radiating elements have exactly same geometry.

All simulations were performed using commercial EM simulation package CST, which is based on Finite Integration Methods [23].

3. RESULTS AND DISCUSSIONS

In order to verify the simulation results, the UWB MIMO antenna under consideration was fabricated, and its prototype version is shown in Figure 6. To validate software pretended results, measurements were performed to measure S -parameters, radiation patterns, gain and performance related MIMO parameters such as Diversity Gain (DG) and Envelope Correlation Coefficient (ECC). The antenna performance matrices are discussed in Section 3.1 while MIMO performance parameters are discussed in Section 3.2.

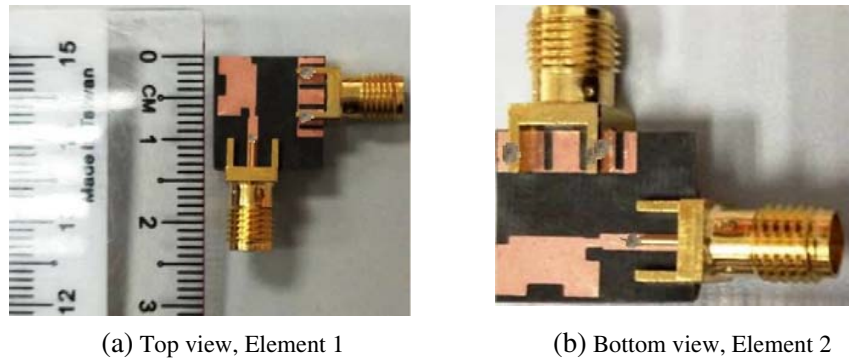


Figure 6. Prototype of the proposed UWB MIMO antenna.

3.1. Antenna Performance

This section includes antenna performance parameters. The S -parameter results are shown in Figure 7. From Figure 7, it can be noticed that measured and software predicted results match very well. As the two radiators are identical with similar ground planes (S_{11} is similar to S_{22}), Figure 7 only shows S_{11} and S_{21} . The bandwidth of impedance provided by the antenna under discussion is 10 GHz (2 GHz–12 GHz), with an isolation of -10 dB throughout the operating band, which is well accepted for a standard MIMO system [24, 25].

Figures 8 and 9 show 2-D radiation plots (E and H -plane) of the proposed UWB MIMO antenna at 3 GHz, 7 GHz and 12 GHz for both elements. Figure 8 presents the simulated and measured radiation patterns of antenna element 1 and antenna element 2 in E plane at 3 GHz, 7 GHz and 12 GHz, whereas

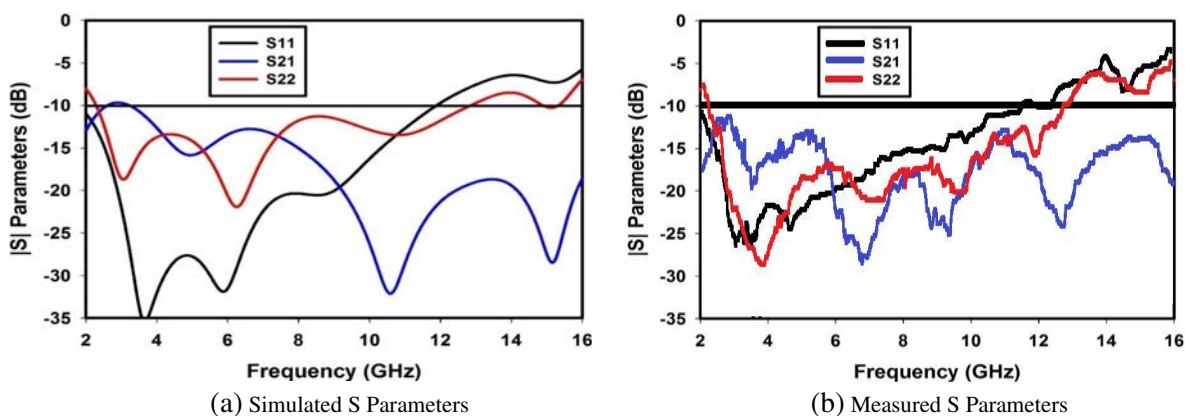


Figure 7. (a) Simulated and (b) measured S -parameters.

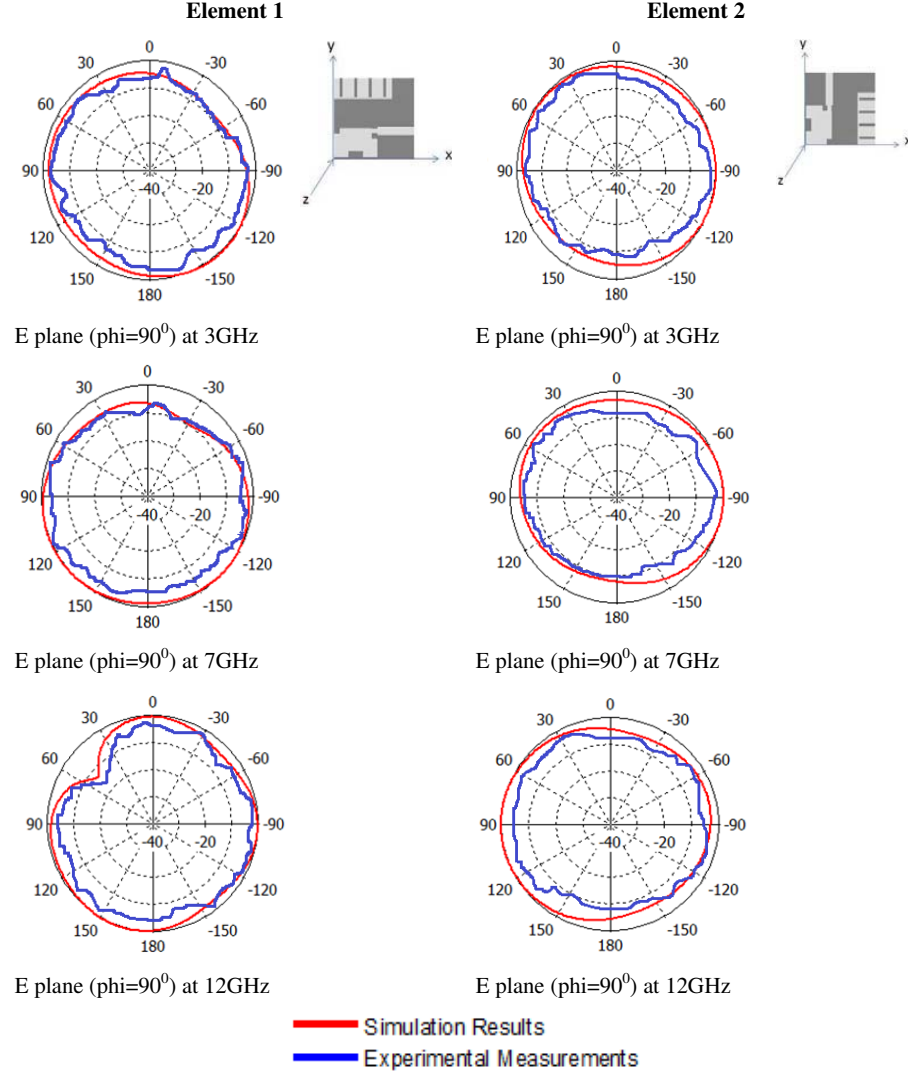


Figure 8. Simulated and measured radiation patterns E plane.

Figure 9 presents the simulated and measured radiation patterns of antenna element 1 and element 2 in H plane at the above-mentioned frequencies.

As clear from both Figures 8 and 9, the designed antenna system elements show nearly omnidirectional radiation pattern pertaining to the whole frequency range. The gain factor of the antenna is presented in Figure 10. The measured gain factor values at frequencies 3 GHz, 7 GHz and 12 GHz are 1.8 dB, 2.8 dB and 4.5 dB, respectively.

3.2. MIMO Performance Parameters

The parameters related to diversity performance of the suggested UWB MIMO antenna in terms of Diversity Gain (DG) and Envelope Correlation coefficient (ECC) are presented in this section.

3.2.1. Envelope Correlation Coefficient (ECC)

The correlation among the MIMO system branches is described by correlation coefficient, and the root of correlation coefficient is the Envelope Correlation Coefficient. ECC can be calculated by using 3-D radiation pattern (pattern Equation (2)) [26] and S -parameters (Equation (3)) [27]. In this paper simulated and measured ECCs are calculated by using Equation (3). The ECC is shown in Figure 11.

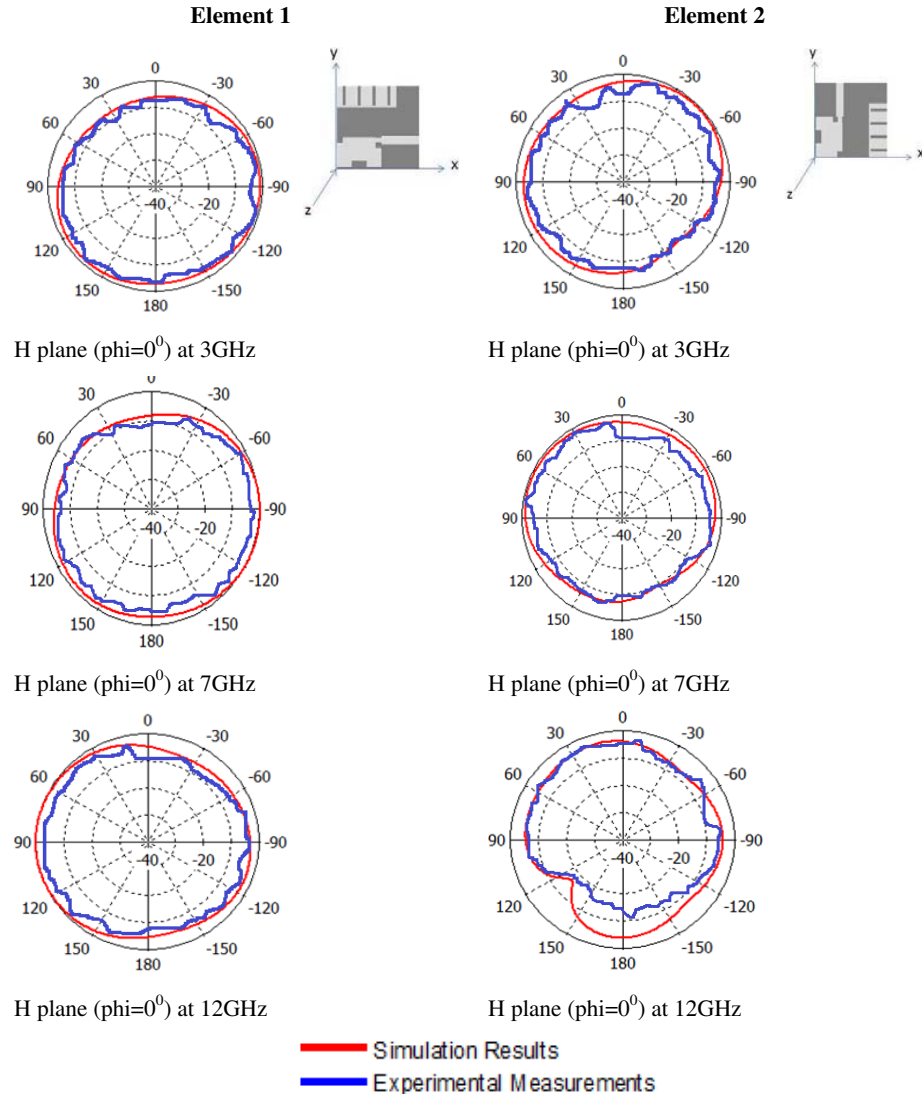


Figure 9. Simulated and measured radiation patterns in H plane.

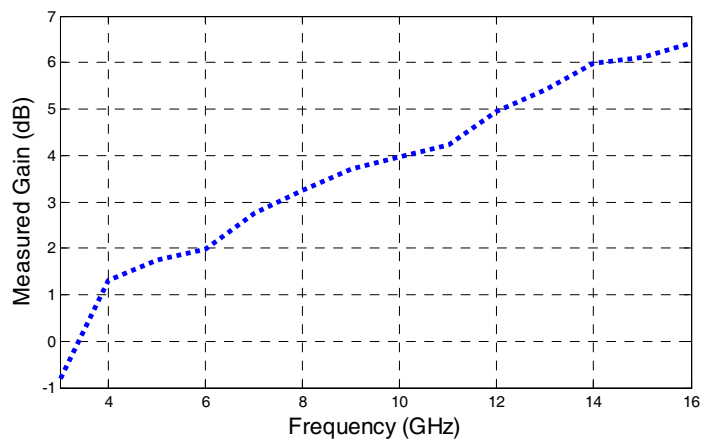


Figure 10. Measured gain of the proposed UWB MIMO antenna.

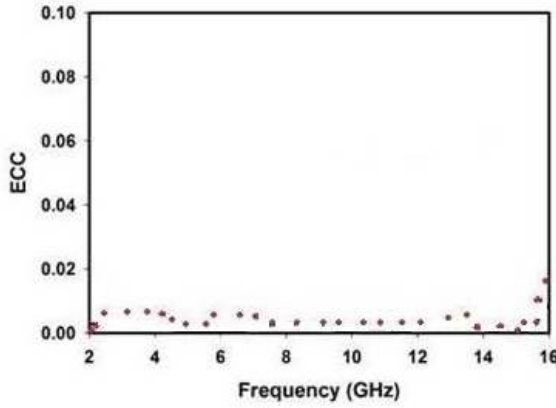


Figure 11. Measured envelop correlation coefficient.

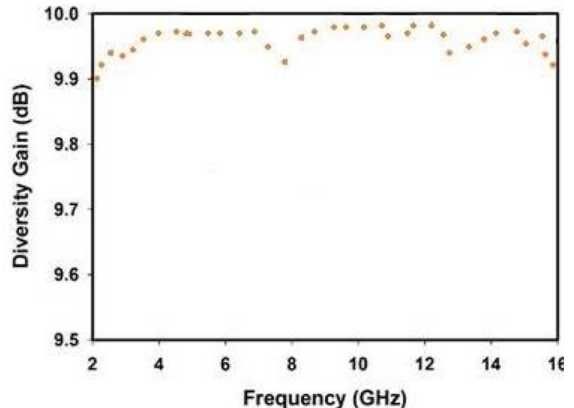


Figure 12. Measured diversity gain.

In the chosen frequency band the ECC has been observed well below 0.5, which is an indication to good diversity enactment [24, 28].

$$\rho_e = \frac{\left| 4\pi F_1^{\rightarrow *}(\theta, \varphi) \cdot F_2^{\rightarrow *}(\theta, \varphi) d\Omega \right|^2}{4\pi \left| F_1^{\rightarrow *}(\theta, \varphi) \right|^2 d\Omega 4\pi \left| F_2^{\rightarrow *}(\theta, \varphi) \right|^2 d\Omega} \quad (2)$$

Under the excited port condition $F_i^{\rightarrow *}(\theta, \varphi)$ is the field radiation pattern of antenna system, and “.” is regarded as Hermitian product.

$$\rho_e = \frac{|S_{11}^* S_{12} + S_{21}^* S_{22}|^2}{\left(1 - (|S_{11}|^2 + |S_{21}|^2)\right) \left(1 - (|S_{22}|^2 + |S_{12}|^2)\right)} \quad (3)$$

The measured significance value for ECC is 0.054 at 2.6 GHz, as shown in Figure 11.

3.2.2. Diversity Gain (DG)

Diversity gain or apparent diversity gain (G_{app}) determines the extent of improvement gained by using a multiple antenna system as compared to a single antenna system. In this study the diversity gain was calculated by using Eq. (4) [24, 29].

$$e_\rho = \sqrt{\left(1 - |0.99\rho_e|^2\right)} \quad \left. \begin{aligned} G_{app} &= 10e_\rho \\ \end{aligned} \right\} \quad (4)$$

Figure 12 shows the measured DG value of suggested antenna. The value of G_{app} is almost 10 dB at the required frequency band, which assures excellent MIMO enactment.

4. CONCLUSION

A new cross polarized 2×2 UWB-MIMO antenna system has been presented in this paper. The prototype antenna system was designed and fabricated. Antenna parameters such as radiation patterns, peak gain, ECC and gain diversity for the designed system have been simulated with software and measured. This UWB-MIMO antenna system consists of two ‘F’ shaped structures with a slotted-fractured ground plane, and the two elements are fabricated back to back cross polarized to each other. The presented MIMO antenna system has very compact size, and the overall volume is $14 \times 14 \times 0.25$ mm³. The overall fractional bandwidth of antenna system was measured as 141.5%. This value fulfills its ultra-wideband response. Also the peak gain value of the antennas system is measured as 4.8 dB. A good agreement was attained between measured and simulated results for prototype design.

ACKNOWLEDGMENT

The authors would like to thank University of Hail, represented by the deanship of scientific research for funding this project (BA-1512).

REFERENCES

1. Maccartney, G. R., T. S. Rappaport, S. Sun, and S. Deng, "Indoor office wideband millimeter-wave propagation measurements and channel models at 28 and 73 GHz for ultra-dense 5G wireless networks," *IEEE Access*, Vol. 3, 2388–2424, 2015, doi: 10.1109/ACCESS.2015.2486778.
2. Ndip, I., T. H. Le, O. Schwanitz, and K.-D. Lang, "A comparative analysis of 5G mmWave antenna arrays on different substrate technologies," *22nd International Microwave and Radar Conference (MIKON) 2018*, 222–225, 2018.
3. Mao, C.-X., S. Gao, and Y. Wang, "Broadband high-gain beam-scanning antenna array for millimeter-wave applications," *IEEE Transactions on Antennas and Propagation*, Vol. 65, No. 9, 4864–4868, 2017.
4. AL-Saif, H., M. Usman, M. T. Chughtai, and J. Nasir, "Compact ultra-wide band MIMO antenna system for lower 5G bands," *Wireless Communications and Mobile Computing*, Vol. 2018, Article ID 2396873, 6 pages, 2018, <https://doi.org/10.1155/2018/2396873>.
5. Matinmikko, M., M. Latva-aho, P. Ahokangas, and V. Seppänen, "On regulations for 5G: Micro licensing for locally operated networks," *Telecommunications Policy*, Vol. 42, No. 8, 622–635, 2018, ISSN 0308-5961, <https://doi.org/10.1016/j.telpol.2017.09.004>.
6. Marsden, R. and H.-M. Ihle, "Mechanisms to incentivise shared-use of spectrum," *Telecommunications Policy*, Vol. 42, No. 4, 315–322, 2018, ISSN 0308-5961, <https://doi.org/10.1016/j.telpol.2017.07.001>.
7. Dighriri, M., G. M. Lee, and T. Baker, "Measurement and classification of smart systems data traffic over 5G mobile networks," *Technology for Smart Futures*, M. Dastbaz, H. Arabnia, and B. Akhgar (eds.), Publisher Springer, Cham, 2018, ISBN 978-3-319-60136-6, https://doi.org/10.1007/978-3-319-60137-3_9.
8. Li, S., D. Xu, and S. Zhao, "5G internet of things: A survey," *Journal of Industrial Information Integration*, Vol. 10, 1–9, 2018, ISSN 2452-414X, <https://doi.org/10.1016/j.jii.2018.01.005>.
9. Wu, Y., K. Ding, B. Zhang, J. Li, D. Wu, and K. Wang, "Design of a compact UWB MIMO antenna without decoupling structure," *International Journal of Antennas and Propagation*, Vol. 2018, Article ID 9685029, 7 pages, 2018, <https://doi.org/10.1155/2018/9685029>.
10. Wang, F., Z. Duan, S. Li, Z.-L. Wang, and Y.-B. Gong, "Compact UWB MIMO antenna with metamaterial-inspired isolator," *Progress In Electromagnetics Research C*, Vol. 84, 61–74, 2018.
11. Wu, L., Y. Xia, X. Cao, and Z. Xu, "A miniaturized UWB-MIMO antenna with quadruple band-notched characteristics," *International Journal of Microwave and Wireless Technologies*, 1–8, 2018, doi:10.1017/S1759078718000508.
12. Usman, M., et al., "New compact dual polarised dipole antenna for MIMO communications," *2010 International ITG Workshop on Smart Antennas (WSA)*, 326–330, Bremen, 2010, doi: 10.1109/WSA.2010.5456429.
13. Malviya, L., R. Panigrahi, and M. Kartikeyan, "MIMO antennas with diversity and mutual coupling reduction techniques: A review," *International Journal of Microwave and Wireless Technologies*, Vol. 9, No. 8, 1763–1780, 2017, doi:10.1017/S1759078717000538.
14. Usman, M., R. A. Abd-Alhameed, and P. S. Excell, "Design considerations of MIMO antennas for mobile phones," *PIERS Online*, Vol. 4, No. 1, 121–125, 2008.
15. Hong, J.-K., "Performance analysis of dual-polarized massive MIMO system with human-care IoT devices for cellular networks," *Journal of Sensors*, Vol. 2018, Article ID 3604520, 8 pages, 2018, <https://doi.org/10.1155/2018/3604520>.

16. Jo, O., J. Kim, J. Yoon, D. Choi, and W. Hong, "Exploitation of dual-polarization diversity for 5G millimeter-wave MIMO beam-forming systems," *IEEE Transactions on Antennas and Propagation*, Vol. 65, No. 12, 6646–6655, Dec. 2017, doi: 10.1109/TAP.2017.2761979.
17. Gao, C., X. Q. Li, W. J. Lu, and K. L. Wong, "Conceptual design and implementation of a four-element MIMO antenna system packaged within a metallic handset," *Microw. Opt. Technol. Lett.*, Vol. 60, 436–444, 2018, <https://doi.org/10.1002/mop.30978>.
18. Al-Hadi, A. A., J. Ilvonen, R. Valkonen, and V. Viikari, "Eight-element antenna array for diversity and MIMO mobile terminal in LTE 3500 MHz band," *Microw. Opt. Technol. Lett.*, Vol. 56, 1323–1327, 2014, doi:10.1002/mop.28316.
19. Li, Y., C. Sim, Y. Luo, and G. Yang, "12-port 5G massive MIMO antenna array in sub-6 GHz mobile handset for LTE bands 42/43/46 applications," *IEEE Access*, Vol. 6, 344–354, 2018, doi: 10.1109/ACCESS.2017.2763161.
20. Li, M., et al., "Eight-port orthogonally dual-polarized antenna array for 5G smartphone applications," *IEEE Transactions on Antennas and Propagation*, Vol. 64, No. 9, 3820-3830, Sep. 2016, doi: 10.1109/TAP.2016.2583501.
21. Thomas, K. G. and M. Sreenivasan, "A simple ultrawideband planar rectangular printed antenna with band dispensation," *IEEE Transactions on Antennas and Propagation*, Vol. 58, 27–34, 2010.
22. Chandel, R., A. K. Gautam, and K. Rambabu, "Tapered fed compact UWB MIMO-diversity antenna with dual band-notched characteristics," *IEEE Transactions on Antennas and Propagation*, Vol. 66, No. 4, 1677–1684, Apr. 2018, doi: 10.1109/TAP.2018.2803134.
23. "CST: Microwave Studio based on the finite integration technique".
24. Zhang, S., K. Zhao, Z. Ying, and S. He, "Adaptive quad-element multi-wideband antenna array for user-effective LTE MIMO mobile terminals," *IEEE Transactions on Antennas and Propagation*, Vol. 61, No. 8, 4275–4283, Aug. 2013, doi: 10.1109/TAP.2013.2260714.
25. Rasilainen, K., A. Lehtovuori, A. Boussada, and V. Viikari, "Carrier aggregation compatible mimo antenna for LTE handset," *Progress In Electromagnetics Research C*, Vol. 78, 1–10, 2017.
26. Vaughan, R. G. and J. B. Andersen, "Antenna diversity in mobile communications," *IEEE Transactions on Vehicular Technology*, Vol. 36, 149–172, 1987.
27. Nasir, J., M. H. Jamaluddin, M. Khalily, M. R. Kamarudin, I. Ullah, and R. Selvaraju, "A reduced size dual port MIMO DRA with high isolation for 4G applications," *International Journal of RF and Microwave Computer Aided Engineering*, Vol. 25, 495–501, 2015.
28. Lee, W. C., *Mobile Communications Engineering*, McGraw-Hill Professional, 1982.
29. Rosengren, K. and P.-S. Kildal, "Radiation efficiency, correlation, diversity gain and capacity of a six-monopole antenna array for a MIMO system: Theory, simulation and measurement in reverberation chamber," *IEE Proceedings-Microwaves, Antennas and Propagation*, Vol. 152, 7–16, 2005.